ACCOUNTS
of chemical research

Organic Molecules as Tools To Control the Growth, Surface Structure, and Redox Activity of Colloidal Quantum Dots

EMILY A. WEISS*

Department of Chemistry, Northwestern University, Evanston, Illinois 60208-3113, United States

RECEIVED ON MARCH 18, 2013

CONSPECTUS

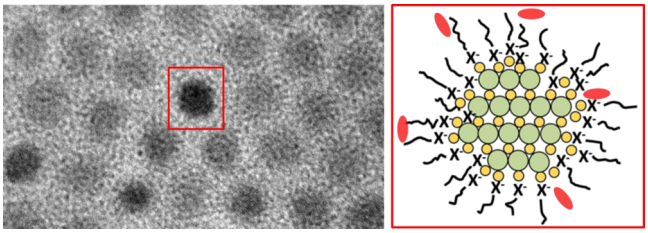

In order to achieve efficient and reliable technology that can harness solar energy, the behavior of electrons and energy at interfaces between different types or phases of materials must be understood. Conversion of light to chemical or electrical potential in condensed phase systems requires gradients in free energy that allow the movement of energy or charge carriers and facilitate redox reactions and dissociation of photoexcited states (excitons) into free charge carriers. Such free energy gradients are present at interfaces between solid and liquid phases or between inorganic and organic materials. Nanostructured materials have a higher density of these interfaces than bulk materials. Nanostructured materials, however, have a structural and chemical complexity that does not exist in bulk materials, which presents a difficult challenge: to lower or eliminate energy barriers to electron and energy flux that inevitably result from forcing different materials to meet in a spatial region of atomic dimensions.

Chemical functionalization of nanostructured materials is perhaps the most versatile and powerful strategy for controlling the potential energy landscape of their interfaces and for minimizing losses in energy conversion efficiency due to interfacial structural and electronic defects. Colloidal quantum dots are semiconductor nanocrystals synthesized with wet-chemical methods and coated in organic molecules. Chemists can use these model systems to study the effects of chemical functionalization of nanoscale organic/inorganic interfaces on the optical and electronic properties of a nanostructured material, and the behavior of electrons and energy at interfaces. The optical and electronic properties of colloidal quantum dots have an intense sensitivity to their surface chemistry, and their organic adlayers make them dispersible in solvent. This allows researchers to use high signal-to-noise solution-phase spectroscopy to study processes at interfaces.

In this Account, I describe the varied roles of organic molecules in controlling the structure and properties of colloidal quantum dots. Molecules serve as surfactant that determines the mechanism and rate of nucleation and growth and the final size and surface structure of a quantum dot. Anionic surfactant in the reaction mixture allows precise control over the size of the quantum dot core but also drives cation enrichment and structural disordering of the quantum dot surface. Molecules serve as chemisorbed ligands that dictate the energetic distribution of surface states. These states can then serve as thermodynamic traps for excitonic charge carriers or couple to delocalized states of the quantum dot core to change the confinement energy of excitonic carriers. Ligands, therefore, in some cases, dramatically shift the ground state absorption and photoluminescence spectra of quantum dots. Molecules also act as protective layers that determine the probability of redox processes between quantum dots and other molecules. How much the ligand shell insulates the quantum dot from electron exchange with a molecular redox partner depends less on the length or degree of conjugation of the native ligand and more on the density and packing structure of the adlayer and the size and adsorption mode of the molecular redox partner.

Control of quantum dot properties in these examples demonstrates that nanoscale interfaces, while complex, can be rationally designed to enhance or specify the functionality of a nanostructured system.

Published on the Web 06/04/2013 www.pubs.acs.org/accounts
10.1021/ar400078u

The behavior of electrons and energy at interfaces between different types or phases of materials is an active research area of both fundamental and technological importance. Such interfaces often result in sharp free energy gradients that provide the thermodynamic driving force for some of the most crucial processes for energy conversion: migration of energy and charge carriers, conversion of excited states to mobile charge carriers, and redox-driven chemical reactions.[1] Nanostructured materials are defined by high surface area-to-volume ratios and should therefore be ideal for the job of energy conversion; however, they have a structural and chemical complexity that does not exist in bulk materials, which presents a formidable challenge: to mitigate or eliminate energy barriers to electron and energy flux that inevitably result from forcing dissimilar materials to meet in a spatial region of atomic dimensions. Chemical functionalization of nanostructured materials is perhaps the most versatile and powerful strategy for controlling the potential energy landscape of their interfaces and for minimizing losses in energy conversion efficiency due to interfacial structural and electronic defects.

Colloidal semiconductor nanocrystals, or quantum dots (QDs), are excellent model systems for fundamental studies of the behavior of electrons at interfaces as a function of interfacial chemistry. Their optical and electronic properties have an intense sensitivity to their surface chemistry,[2,3] and their organic adlayers make them dispersible in solvent, which allows us to use high signal-to-noise solution-phase spectroscopy to study processes at interfaces. In order to map the properties of a QD/molecule system to its interfacial structure, it is useful to divide nanoparticle−molecule interactions into three categories: physisorbed surfactant, chemisorbed ligands electronically coupled only to local surface ions, and chemisorbed ligands electronically coupled nonperturbatively to the band structure of the QD core; ligands in the latter category change the confinement potential for excitonic carriers. In each category, the ligand serves a particular function or set of functions: imparting solubility to the QDs in a selected solvent, preventing particle aggregation, electronically passivating surfaces to enhance, for example, photoluminescence yield, or controlling the coherence length and energy of the exciton.

Herein are a few examples that demonstrate the power of tuning the chemistry at the organic−inorganic interface within colloidal QDs as a strategy for controlling their structure and properties. We focus on the role of molecules as surfactant during the QDs' nucleation and growth and as ligands that dictate the chemical and electronic structure of the interfacial region, and we outline mechanisms by which this structure determines the fate of the QD's excited state and its ability to exchange electrons with proximate redox partners. We hope to illustrate that even complex nanoscale organic/inorganic interfaces can be designed rationally in order to enhance or specify the functionality of a nanostructured system.

Control of QD Nucleation and Growth

The role of organic molecules in determining the properties of a QD starts in the reaction mixture. For metal-chalcogenide QDs (like CdS or CdSe), one strategy for precise control of QD growth is to use a highly reactive chalcogenide precursor to rapidly nucleate a collection of small semiconductor clusters.[4,5] For instance, the reaction of diphenylphosphine selenide and a cadmium-carboxylate results in 100% nucleation in less than five minutes at room temperature, whereas the typical precursor trioctylphosphine selenide takes tens of minutes to react fully with a cadmium-carboxylate precursor at 300 °C.[4] Once nucleation occurs, there exists a population of clusters that, at room temperature, are stable to dissolution or further reaction. The clusters are a type of reagent that can be isolated and used later or created *in situ* in the same "pot" in which the nanocrystals grow.

The clusters have two possible growth pathways. The first is combination of the small clusters to form "oligomers" that are integer multiple volumes of the base unit, a process directly analogous to step-addition polymerization.[6−9] We can force the clusters down this growth pathway if we heat them in the *absence* of excess anionic ligand, Figure 1A. We suspect that fusion of clusters by step-growth polymerization is an explanation for the consistent observation of certain sizes of clusters during the growth of QDs, over many years in many laboratories,[8,10−13] an observation sometimes attributed to exceptional thermodynamic stability of certain clusters (i.e., they are "magic-sized").[11,14−17]

In the second mechanism, a portion of the small clusters dissolve to produce "monomer" that feeds $n \rightarrow n + 1$ growth of other clusters in the population, a process directly analogous to living chain addition polymerization.[6,7,9] We choose this growth pathway if we heat the clusters in the *presence* of excess anionic ligand (we have found the conjugate bases of carboxylic or phosphinic acids to be effective and convenient), Figure 1B. Chain growth is a controlled Ostwald ripening.[18] We refer to this process as a "living" chain addition because it has no explicit termination step; growth saturates when the molecular feedstock (or "monomer") produced by dissolution of

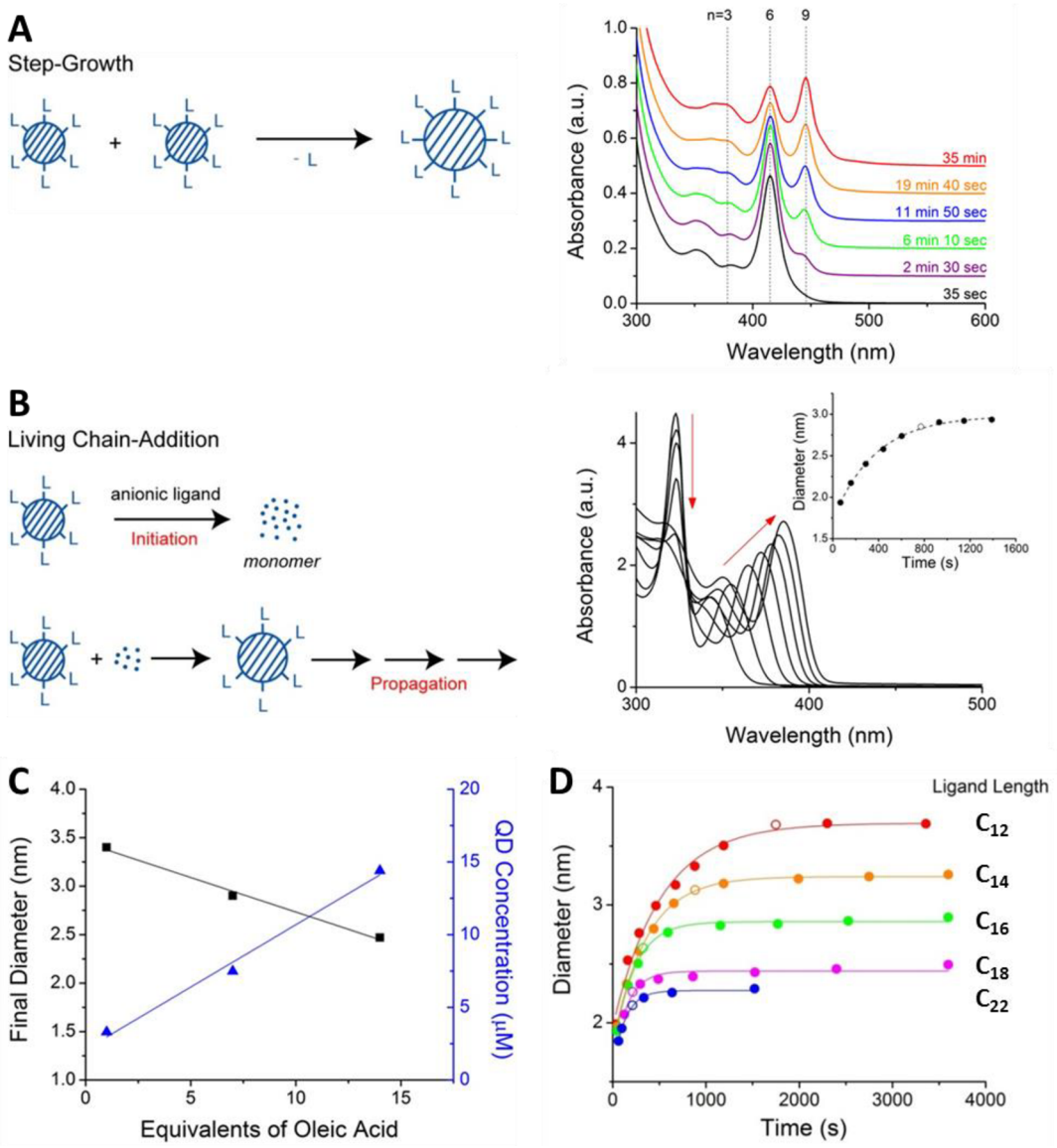

FIGURE 1. Surfactant-controlled mechanisms of QD growth. (A) Step-growth mechanism for nanocrystal growth and spectra for clusters heated in oleylamine at 200 °C. The vertical lines show the positions of peaks for clusters that have integer multiples of the volume of the smallest cluster observed. (B) Living chain addition mechanism for nanocrystal growth and absorption spectra of CdS grown at 185 °C in excess oleic acid. The QD diameter reaches a maximum shortly after the disappearance of the peak at 323 nm (inset, open circle), which corresponds to the cluster. (C) For CdS produced at 185 °C with varying amounts of oleic acid, the final diameter of QDs (squares) is inversely related to the concentration of added oleic acid, while QD concentration (triangles) has the reverse trend. (D) Increasing chain length of the carboxylic acid ligand leads to a larger population of "stable" clusters that eventually grow into a larger population of QDs with a smaller diameter. Adapted from ref 6.

the less-stable clusters runs out. This natural saturation of size is the advantage of growing QDs with the chain-addition mechanism rather than through step-addition or nonclusterinitiated synthesis, because the point in the growth trajectory at which the cluster dissolution ceases depends entirely on how many clusters within the initial population are "stable" (and therefore form nuclei for eventual nanocrystals) and how many are "unstable" (and therefore dissolve). This branching ratio is determined by precisely controllable parameters like the molar ratio of anionic surfactant to the limiting ionic reagent (Se^{2-} or S^{2-}) (Figure 1C) or the chain length of the anionic ligand (Figure 1D).[6]

The size and shape of nanocrystals and their degree of crystallinity is dramatically sensitive to the chemical structure of any coordinating ligand present in the reaction mixture. This sensitivity is advantageous in designing strategies for synthesizing, for example, zero-, one-, or two-dimensional crystals of a given semiconductor[19] but also means that even minor impurities in starting materials lead to irreproducibility in the structure of the product.[20]

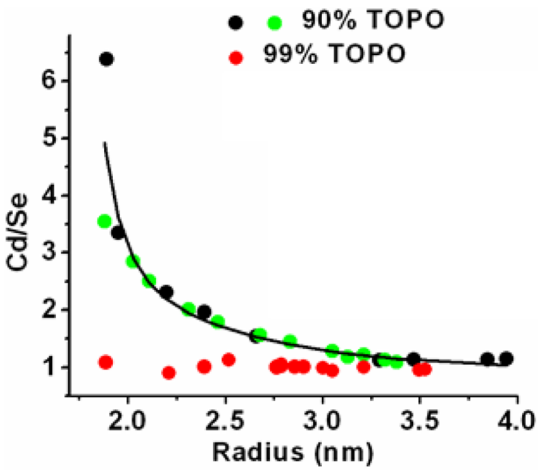

FIGURE 2. Surfactant-driven cadmium enrichment of CdSe QDs. ICP-AES-measured Cd/Se ratios within QDs synthesized in reagent-grade TOPO, which contains acid impurities (black, green), and in 99% TOPO (red). Adapted from ref 22.

The living chain addition polymerization allows for control of QD radius through pure organic reagents[20] without relying on reaction time or temperature.

Anionic Surfactant Controls the Composition of the QD Surface

Quantum dots grown in the presence of anionic surfactant, either as a prescribed component of the reaction mixture (as in the procedure outlined above) or as anionic impurities in reagent-grade trioctylphosphine oxide (TOPO),[20,21] the most common coordinating solvent for CdSe growth, are capped primarily by these negatively charged, so-called "X-type" ligands after synthesis and purification.[22−25] A combination of analytical techniques, including X-ray photoelectron spectroscopy and ^{31}P NMR, allowed us to determine that more than 80% of the atoms on the surfaces of CdSe QDs synthesized in reagent-grade TOPO are coated by alkylphosphonates that are known TOPO impurities.[20,21,23] Few if any of the datively bound surfactants hexadecylamine, TOPO, and trioctylphosphine selenide are present. The inorganic portion of the interfacial region of the QD is therefore enriched with charge-balancing cations (Cd^{2+}).

The cation enrichment of the QD at the inorganic/organic interface, even after precipitation, can be extreme, depending on the concentration of anionic surfactant used in the synthesis and the final size of the QD. We measured with ICP-AES that the ratio of Cd to Se within colloidal CdSe QDs increases from 1.2:1 for QDs with radius of 3.3 nm to 6.5:1 for a radius of 1.9 nm, Figure 2.[22] In the absence of anionic surfactant in the reaction mixture, the molar ratio Cd/Se ≈ 1:1 for all sizes. Cation enrichment of the QDs is therefore driven by strongly bound alkylphosphonates that stabilize the interface between the polar CdSe core and the organic solvent.

The presence of cadmium−phosphonate complexes on the surface of the QD creates structural disorder within both the organic and inorganic components of the interface. Sum frequency generation (SFG) studies of alkylphosphonate adlayers of CdSe QDs indicate that the density of *gauche* defects in these layers, which is a measure of their conformational disorder, increases as the radius of the QD decreases.[26] This increase in disorder is not accounted for completely by the increase in the curvature of the nanoparticle with decreasing size (a model that explains trends in SFG spectra of organic adlayers on gold nanoparticles with size).[27] In addition to geometric effects, the disorder in adlayers on CdSe QDs originates from structural disordering of the underlying Cd^{2+}, which manifests as broadening of Cd lines in the XPS spectrum of the sample.

Although reaction mixtures rich in anionic ligand produce nonstoichiometric and, in the case of CdSe, structurally disordered surfaces, these ligands offer synthetic control of size, shape, and surface composition that one does not obtain using dative ligands as the primary surfactant.[20] If, as we describe above, the anionic surfactant is used in known quantities, as opposed to added as an impurity whose concentration varies from synthetic batch to synthetic batch, and the QD structure is chemically analyzed post-synthesis, the organic/inorganic interface is a known, controllable input parameter in modeling the physical properties of the QD. Notably, successive ionic layer adsorption and reaction (SILAR) and related procedures allow for selective enrichment of QD surfaces with either cations or anions in order to control, for example, the photoluminescence energy and quantum yield of the QD.[28]

Influence of Ligands on the Absorption and Photoluminescence of QDs

Control and quantitative characterization of the chemical structure of the surface of a QD is a necessary step toward making them optically functional materials, because the orbitals of chemisorbed ligands contribute to density of states in the interfacial region that potentially determines both static and dynamic properties of the QD's excited state, or "exciton".[29,30]

When the frontier orbitals of the ligand are energetically resonant with, and have common symmetry to, states within the semiconductor band of the QD core, the electronic structure of the organic/inorganic interface determines the

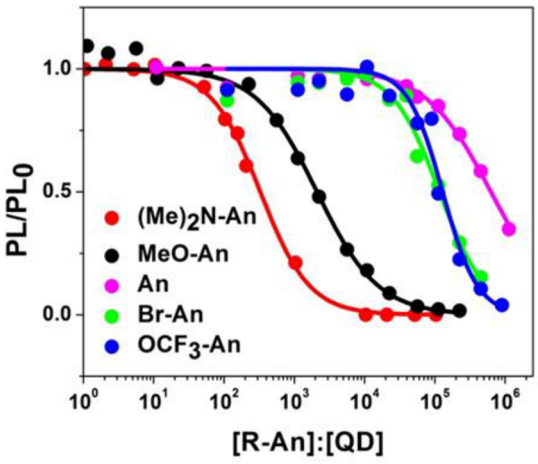

FIGURE 3. Quenching of PL of CdSe QDs with substituted anilines. The ratio of the PL intensity of CdSe QD/R-An mixtures and the PL intensity of QDs before addition of anilines (PL_0) vs [R-An]/[QD]. Reprinted from ref 40. Copyright 2010 American Chemical Society.

confinement potential for the exciton and therefore the energy of the lowest excited state of the QD. The class of ligands phenyldithiocarbamates couples electronically to the delocalized states of CdSe, CdS, and PbS QDs to reduce the optical band gap of the QDs by up to 1 eV, by relaxing the quantum confinement of excitonic carriers. We describe the mechanism of this interaction in detail elsewhere.[31−34] Even if the frontier orbitals of a chemisorbed ligand are not of the correct energy or symmetry to perturb the steady-state properties of the QD by redefining its band edges, the ligand potentially introduces mid-bandgap states that are thermodynamically accessible to the excitonic electron or hole.[35,36] Such mid-bandgap states, or "traps", provide pathways for decay of delocalized excitonic states into states where one or both carriers are localized on a surface ion or group of ions. Ligands influence the spatial and energetic distribution of trap states either by explicitly providing them (for example, lone pairs on the sulfur headgroups of thiolate ligands are thermodynamic traps for excitonic holes of CdSe QDs[36]) or by serving as electronic passivators.[37] Passivating ligands exchange electron density with incompletely coordinated metal or chalcogenide ions that would otherwise be traps themselves. Many of the chemical strategies and descriptive models for passivation of nanocrystal surfaces derive from extensive work on the response of the photoluminescence of bulk single crystals of CdS and CdSe to charge-transfer interactions at the interfaces of these crystals with small molecules.[38,39] When a "good" passivator (like an electron-donating alkylamine) is replaced with a weaker electron donor (like aniline), the photoluminescence of the QD is quenched.[40] The relationship of the photoluminescence of a QD and the concentration of an added ligand is a complicated function that reflects the surface coverage of the ligand and the competition between radiative and trapping processes.[41] We observed, for instance, that the dependence of the PL of a sample of CdSe QDs on the concentration of added aniline ligands requires a model that includes two functions, a binding isotherm and a function that describes the response of the PL to R-An ligands once they are bound at their equilibrium surface coverage, and that we could tune the overall response with simple substitutions of the aniline at the *para* position of the phenyl ring, Figure 3.[40]

Trapping of one or both carriers from the band-edge exciton does not necessarily quench the PL of the QD. Some of these trapped carriers, especially if localized on surface ions[28] and not ligand orbitals, are still part of emissive excitons[42,43] with energies indistinguishable from that of band-edge emission or shifted to lower energy by more than 100 nm (so-called "defect emission").

The Ligand Shell of a QD Dictates Its Redox Activity

The intra- and intermolecular structure of the native (as-synthesized) ligands of the QD determines its tendency to exchange electrons with proximate redox centers. Given a thermodynamically "downhill" electron transfer (eT) reaction, the ligand shell dictates the electronic coupling and therefore the reaction rate.[44] We have found that, for the long-chain saturated or mono-unsaturated organic ligands most common as native ligands for QDs, a redox-active molecule must approach the QD surface through "gaps" in the ligand shell in order to participate in charge transfer with the QD. The degree to which the ligand shell insulates the QD thus depends less on the length or degree of conjugation of the ligand and more on its density and packing structure and the size and adsorption mode of the molecular redox partner.[45,46]

The influence of a QD's ligand shell on the efficiency by which a QD exchanges electrons with molecules is very apparent in an experiment we performed with CdS QDs (as the electron donor) and an acid-derivatized viologen (as the electron acceptor).[47] The observable in this experiment is the PL intensity of the QD sample: if a viologen molecule achieves what we call an "electron-transfer active configuration" on the surface of the QD, the electron transfer is fast enough (single picoseconds) to quantitatively out-compete radiative recombination of the exciton.[48] We found that, as expected, the higher the molar ratio of viologen quencher to QD in the sample, the less emission we observed from the QDs.

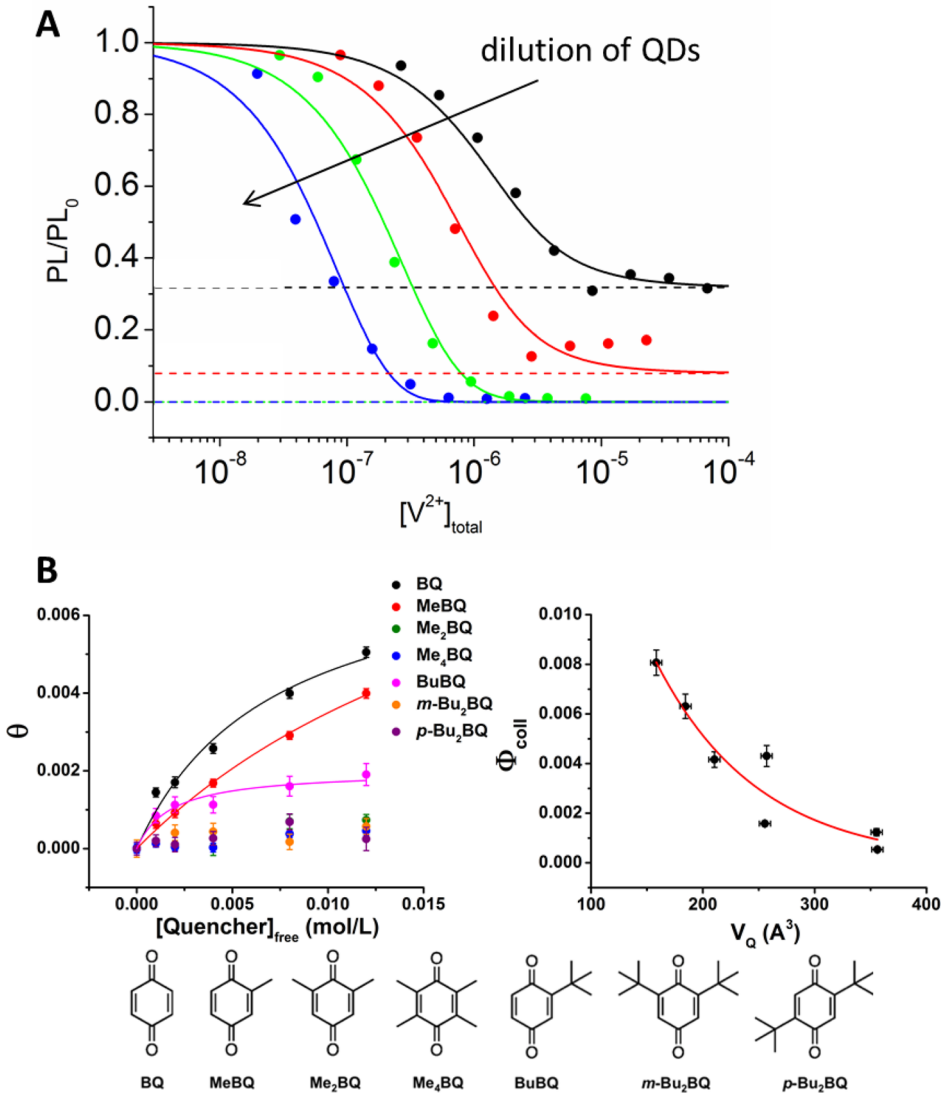

FIGURE 4. (A) Electron transfer from CdS QDs to viologen. PL intensity with added viologen, divided by PL intensity without added viologen (PL/PL_0) vs the total concentration of added viologen for samples of 1.4×10^{-6} M (black), 4.6×10^{-7} M (red), 1.5×10^{-7} M (green), and 5.1×10^{-8} M (blue) CdS QDs. The solid lines are the best fits to a double binomial function sharing the value of the QD-viologen adsorption constant across all four concentrations. The dashed lines show the probability of finding QDs with zero available adsorption sites. This probability goes to zero with dilution. Adapted from ref 47. (B) Electron transfer from PbS QDs to benzoquinones. (left) Langmuir plots of fractional surface coverage of adsorbed quenchers versus concentration of free quencher molecules for all substituted BQs. The Langmuir plots for Me_2BQ, Me_4BQ, *m*-Bu_2BQ, and *p*-Bu_2BQ show surface coverages near zero for all concentrations. (right) Plot of the collisional quenching efficiency, Φ_{coll}, versus the molecular volume of the alkyl-substituted BQ quenchers, V_Q. Adapted from ref 52.

Unexpected at the time, however, is the result that the response of PL to added viologen depends on the absolute concentration of the QDs and not just the molar ratio of quencher to QD, Figure 4A.[47] We determined that the increase in quenching efficiency upon dilution results from an increase in the mean number of available adsorption sites per QD through desorption of native carboxylate ligands. We therefore developed a new model, based on the work of Tachiya[49] and others,[50] that treats both the number of adsorbed ligands per QD and the number of available binding sites per QD as binomially distributed quantities.[47] This "double binomial" model is necessary for quantitative analysis of electron transfer rates and yields in the presence of native ligands, which themselves are in dynamic equilibrium with the QD surface.

The initial CdS–viologen experiments reveal that (i) QDs have a finite capacity for accommodating redox-active molecules on their surfaces in geometries that permit sufficient electronic coupling for charge transfer, (ii) the native ligand shell is dynamic, and (iii) the shell's imperfections,

whether static or transient, create pathways by which molecules can achieve favorable adsorption geometries. These lessons are enforced and specified further by the interaction of PbS QDs and the photoreductant aminoferrocene (amFc). When comparing the hole transfer rates from the QD to amFc for two types of PbS QDs, one coated with a 1.5-nm-thick adlayer of oleate and another coated with a ~0.8-nm-thick adlayer of decanethiolate, we observed that hole transfer does not occur from the decanethiolate-coated QDs and occurs very quickly (with a time constant on the order of single picoseconds) from the oleate-coated QDs.[46] This result is unexpected if the hole transfer were proceeding by tunneling through the ligand layer and indicates that the hole bypasses the through-bond pathway provided by the native ligands. The redox-active molecule therefore permeates the ligand shell to diffuse to the surface of the QD. We suspect, but have not yet proven, that the oleate shell renders the QD more susceptible to charge transfer because oleate has a smaller adsorption constant than thiolate, such that amFc is able to displace oleate (but not thiolate) from the surface of the QD to achieve a charge transfer-active configuration on the QD surface.

"Open sites" on the QD surface due to defects in the organic adlayer allow for adsorption of redox-active molecules and ultrafast charge transfer, but the formation of quasi-static donor–acceptor complexes is not the only mechanism by which QDs exchange electrons with molecules in solution. If the QD has an exciton lifetime longer than the average intercollision time for the QD–molecule system, it can, in principle, participate in both static and collisionally gated charge transfer, where the structure of the ligand shell dictates the rates and yields of both types of processes. We examined this issue with PbS QDs (which have an excited state lifetime of ~2.5 μs) and a series of substituted benzoquinones.[51,52] 1,4-Benzoquinone (BQ) acts as a photo-oxidant for PbS QDs via two mechanisms: eT from the QD to adsorbed BQ molecules and collisionally gated eT to freely diffusing BQ. The availability of a collisionally gated pathway improves the yield of electron transfer from PbS QDs to BQ by an average factor of 2.5 over that for static electron transfer alone. The size and shape of the BQ molecule influences the probability of both adsorbed and diffusional processes, even after accounting for variation in reduction potential throughout the series. BQs containing more than one alkyl substituent do not participate in static photoinduced eT with PbS QDs because, we suspect, there is not a defect in the ligand shell large enough to create an "empty" adsorption site for these sterically hindered molecules. For the BQs that do participate in static eT, the adsorption

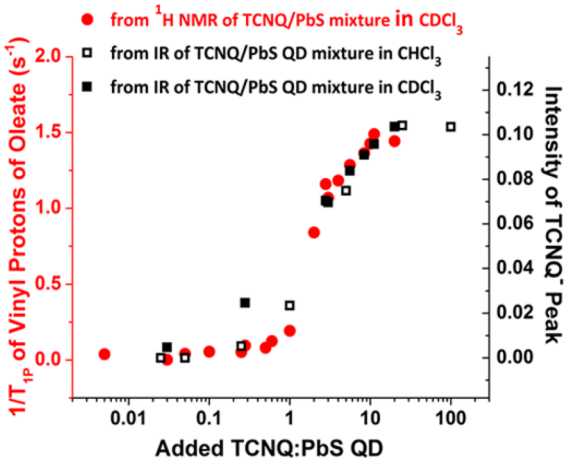

FIGURE 5. Spontaneous multielectron transfer from PbS QD surfaces to TCNQ. (left axis, red) Plot of paramagnetic contribution to the spin–lattice relaxation rate of the spins of vinyl protons (5.3 ppm) of oleate on the surfaces of PbS QDs vs [TCNQ]/[QD]. (right axis, black) Intensity of the peak corresponding to the C–N stretching mode of TCNQ anion vs TCNQ/QDs. The overlap of NMR and IR data sets indicates that electron transfer to TCNQ is responsible for creation of paramagnetic centers at the surface of the QD. Reproduced from ref 45. Copyright 2013 American Chemical Society.

equilibrium constant decreases as the molecular volume of the substituted BQ increases (Figure 4B, left). The efficiency of collisional eT from a PbS QD to a freely diffusing substituted BQ quencher, Φ_{coll}, also decreases as the molecular volume increases (Figure 4B, right). These trends are captured by a model that calculates the free energy of transfer of the molecule from solvent into the ligand shell based on the difference in osmotic pressure in the two phases.[52]

The surface structure dictates the rate and yield of not only photoinduced electron transfer but also spontaneous charge transfer, that is, the tendency of the QD to form multiplexed ground-state CT complexes with easily oxidized or reduced molecules.[45] There are several examples of spontaneous CT involving semiconductor nanoparticles in the literature.[53,54] We studied multielectron ground-state CT complexes of oleate-coated PbS QDs and tetracyanoquinodimethane (TCNQ) in $CHCl_3$. Because this donor–acceptor complex forms indefinitely stable ion pairs, we can characterize the complex with steady-state visible and mid-infrared absorption spectroscopy (to monitor the anion of TCNQ) and NMR spectroscopy of the protons of oleate ligands that coat the QDs. The spin–lattice relaxation rates of these protons increase as charge transfer creates paramagnetic centers at the inorganic/organic interface, Figure 5. We determined that within these complexes, the electron donor is not the QD core but rather a sulfur ion on the surface of the QD and

that, just as with photoinduced eT, the ligand shell of the PbS QDs dictates the set of adsorption geometries available to the TCNQ molecules and the total number of reduced TCNQ molecules per QD. Between one and two TCNQ molecules adsorb directly to the surface of the QDs. After these "empty sites" fill, TCNQ molecules adsorb by displacing of oleate ligands (in the form of lead oleate) from the surface.[45]

In the solid state, the intermolecular structure of the ligand shell is even more important for determining the redox activity of a QD because there is limited energy for conformational changes and no dynamic adsorption equilibrium (whereby a redox-active ligand can displace a native ligand). In a study of the rate of photoinduced eT from CdSe QDs to poly(viologen) within thin films, we observe distinct dependencies of eT rate on the length of the native ligands ($HS\text{-}(CH_2)_n\text{-}COOH$) of the QD in two regimes of monolayer structure.[55] When $n < 10$, the organic adlayer is predicted to be liquid-like (based on the literature on self-assembled monolayers on flat gold and gold nanoparticles[56,57]), and we observe ultrafast eT but with a distance dependence that indicates a collapsed (i.e., *gauche*-defective) ligand shell. When $n \geq 10$, a regime in which the organic adlayer is predicted to be crystalline, the eT rate constants are much slower than those expected based on the trend for $n < 10$. We attribute this change in distance-dependence to the formation of bundles of *trans*-extended ligands that limit access of the viologen units to the surfaces of the QDs, and make eT uncompetitive with radiative recombination of the exciton.

Conclusion

We have presented much of what one might consider to be indirect evidence of the influence of organic ligands in the formation and physical properties of QDs. We and many others are interested in developing methods for obtaining more direct information about how ligands integrate into the chemical structure, electronic structure, and dynamical behavior of a QD. For instance, can we image, dynamically and in three dimensions, the organic−inorganic interface of a 3-nm colloid to determine exactly how a chelating ligand reconstructs the terminal ions of the lattice and whether that ligand is stationary or diffuses along the surface? Can we determine, by monitoring the vibrational dynamics of ligands (rather than inferring from the electronic dynamics of the QDs), how energy dissipates from the exciton into the surrounding medium? This type of knowledge leads to chemical control over nanoscale interfaces that, in turn, allow us to exploit the exceptional light harvesting capabilities of these materials for photochemical catalysis, their unique electronic structure for optical up- and down-conversion processes, or their tunable surfaces for dynamic self-assembly. The transition of the quantum dot field from a collection of interesting fundamental systems to the development of functional materials for energy conversion and other applications has already begun, but there are many critical fundamental chemical problems to solve in order to sustain the field's steep trajectory.

The author would like to thank the Henry Luce Foundation for its support from 2008 to 2013 through a Clare Booth Luce Professorship.

BIOGRAPHICAL INFORMATION

Emily Weiss is the Irving M. Klotz Research Professor of Chemistry at Northwestern University, where she started her independent career in 2008. Her group seeks to understand the mechanisms of energy conversion at interfaces and to design and synthesize nanostructures that are new combinations of organic and inorganic components. Emily is the recipient of young faculty awards from the Department of Energy, the Air Force, and the Packard and Sloan Foundations and of a Presidential Early Career Award for Scientists and Engineers.

FOOTNOTES

*E-mail: e-weiss@northwestern.edu.
The authors declare no competing financial interest.

REFERENCES

1 *Current Challenges in Organic Photovoltaic Solar Energy Conversion*; Schlenker, C. W., Thompson, M. E., Eds.; Springer-Verlag: Heidelberg, Germany, 2011.
2 Bullen, C.; Mulvaney, P. The effects of chemisorption on the luminescence of CdSe quantum dots. *Langmuir* **2006**, *22*, 3007–3013.
3 Jones, M.; Lo, S. S.; Scholes, G. D. Quantitative modeling of the role of surface traps in CdSe/CdS/ZnS nanocrystal photoluminescence decay dynamics. *Proc. Natl. Acad. Sci. U.S.A.* **2009**, *106*, 3011–3016.
4 Evans, C. M.; Evans, M. E.; Krauss, T. D. Mysteries of TOPSe revealed: Insights into quantum dot nucleation. *J. Am. Chem. Soc.* **2010**, *132*, 10973–10975.
5 Owen, J. S.; Chan, E. M.; Liu, H.; Alivisatos, A. P. Precursor conversion kinetics and the nucleation of cadmium selenide nanocrystals. *J. Am. Chem. Soc.* **2010**, *132*, 18206–18213.
6 Evans, C. M.; Love, A. M.; Weiss, E. A. Surfactant-controlled polymerization of semiconductor clusters to quantum dots through competing step-growth and living chain-addition mechanisms. *J. Am. Chem. Soc.* **2012**, *134*, 17298–17305.
7 Odian, G. *Principles of Polymerization*, 4 ed.; John Wiley and Sons: Hoboken, NJ, 2004.
8 Fojtik, A.; Weller, H.; Koch, U.; Henglein, A. Photo-chemistry of colloidal metal sulfides 8. Photo-physics of extremely small CdS particles: Q-state CdS and magic agglomeration numbers. *Ber. Bunsen-Ges. Phys. Chem.* **1984**, *88*, 969–977.
9 Cademartiri, L.; Guerin, G.; Bishop, K. J. M.; Winnik, M. A.; Ozin, G. A. Polymer-like conformation and growth kinetics of Bi_2S_3 nanowires. *J. Am. Chem. Soc.* **2012**, *134*, 9327–9334.
10 Herron, N.; Calabrese, J. C.; Farneth, W. E.; Wang, Y. Crystal structure and optical properties of $Cd_{32}S_{14}(SC_6H_5)_{36}$ DMF_4, a cluster with a 15 angstrom CdS core. *Science* **1993**, *259*, 1426–1428.
11 Peng, Z. A.; Peng, X. Nearly monodisperse and shape-controlled CdSe nanocrystals via alternative routes: Nucleation and growth. *J. Am. Chem. Soc.* **2002**, *124*, 3343–3353.
12 Soloviev, V. N.; Eichhofer, A.; Fenske, D.; Banin, U. Molecular limit of a bulk semiconductor: Size dependence of the "band gap" in CdSe cluster molecules. *J. Am. Chem. Soc.* **2000**, *122*, 2673–2674.

13 Vossmeyer, T.; Reck, G.; Katsikas, L.; Haupt, E. T. K.; Schulz, B.; Weller, H. A "double-diamond superlattice" built up of $Cd_{17}S_4(sSCH_2CH_2OH)_{26}$ clusters. *Science* **1995**, *267*, 1476–1479.

14 Bowers, M. J., II; McBride, J. R.; Rosenthal, S. J. White-light emission from magic-sized cadmium selenide nanocrystals. *J. Am. Chem. Soc.* **2005**, *127*, 15378–15379.

15 Evans, C. M.; Guo, L.; Peterson, J. J.; Maccagnano-Zacher, S.; Krauss, T. D. Ultrabright PbSe magic-sized clusters. *Nano Lett.* **2008**, *8*, 2896–2899.

16 Kudera, S.; Zanella, M.; Giannini, C.; Rizzo, A.; Li, Y.; Gigli, G.; Cingolani, R.; Ciccarella, G.; Spahl, W.; Parak, W. J.; Manna, L. Sequential growth of magic-size CdSe nanocrystals. *Adv. Mater.* **2007**, *19*, 548–552.

17 Wang, Y.; Liu, Y.-H.; Zhang, Y.; Wang, F.; Kowalski, P. J.; Rohrs, H. W.; Loomis, R. A.; Gross, M. L.; Buhro, W. E. Isolation of the magic-size CdSe nanoclusters[$(CdSe)_{13}$-(n-octylamine)$_{13}$] and [$(CdSe)_{13}$(oleylamine)$_{13}$]. *Angew. Chem., Int. Ed.* **2012**, *51*, 6154–6157.

18 Talapin, D. V.; Rogach, A. L.; Haase, M.; Weller, H. Evolution of an ensemble of nanoparticles in a colloidal solution: Theoretical study. *J. Phys. Chem. B* **2001**, *105*, 12278–12285.

19 Wang, F.; Tang, R.; Buhro, W. E. The trouble with TOPO; identification of adventitious impurities beneficial to the growth of cadmium selenide quantum dots, rods, and wires. *Nano Lett.* **2008**, *8*, 3521–3524.

20 Son, J. S.; Park, K.; Kwon, S. G.; Yang, J.; Choi, M. K.; Kim, J.; Yu, J. H.; Joo, J.; Hyeon, T. Dimension-controlled synthesis of CdS nanocrystals: From 0D quantum dots to 2D nanoplates. *Small* **2012**, *8*, 2394–2402.

21 Kopping, J. T.; Patten, T. E. Identification of acidic phosphorus-containing ligands involved in the surface chemistry of CdSe nanoparticles prepared in tri-n-octylphosphine oxide solvents. *J. Am. Chem. Soc.* **2008**, *130*, 5689–5698.

22 Morris-Cohen, A. J.; Frederick, M. T.; Lilly, G. D.; McArthur, E. A.; Weiss, E. A. Organic surfactant-controlled composition of the surfaces of CdSe quantum dots. *J. Phys. Chem. Lett.* **2010**, *1*, 1078–1081.

23 Morris-Cohen, A. J.; Donakowski, M. D.; Knowles, K. E.; Weiss, E. A. The effect of a common purification procedure on the chemical composition of the surfaces of CdSe quantum dots synthesized with trioctylphosphine oxide (TOPO). *J. Phys. Chem. C* **2010**, *114*, 897–906.

24 Jasieniak, J.; Mulvaney, P. From Cd-rich to Se-rich — the manipulation of CdSe nanocrystal surface stoichiometry. *J. Am. Chem. Soc.* **2007**, *129*, 2841–2848.

25 Owen, J. S.; Park, J.; Trudeau, P.-E.; Alivisatos, A. P. Reaction chemistry and ligand exchange at cadmium–selenide nanocrystal surfaces. *J. Am. Chem. Soc.* **2008**, *130*, 12279–12281.

26 Frederick, M. T.; Achtyl, J. A.; Knowles, K. E.; Weiss, E. A.; Geiger, F. M. Surface-amplified ligand disorder in CdSe quantum dots determined by electron and coherent vibrational spectroscopies. *J. Am. Chem. Soc.* **2011**, *133*, 7476–7481.

27 Bordenyuk, A. N.; Weeraman, C.; Yatawara, A.; Jayathilake, H. D.; Stiopkin, I. L., Y.; Benderskii, A. V. Vibrational sum frequency generation spectroscopy of dodecanethiol on metal nanoparticles. *J. Phys. Chem. C* **2007**, *111*, 8925–8933.

28 Wei, H. H.-Y.; Evans, C. M.; Swartz, B. D.; Neukirch, A. J.; Young, J.; Prezhdo, O. V.; Krauss, T. D. Colloidal semiconductor quantum dots with tunable surface composition. *Nano Lett.* **2012**, *12*, 4465–4471.

29 Guyot-Sionnest, P.; Wehrenberg, B.; Yu, D. Intraband relaxation in CdSe nanocrystals and the strong influence of the surface ligands. *J. Chem. Phys.* **2005**, *123*, No. 074709.

30 Knowles, K. E.; Frederick, M. T.; Tice, D. B.; Morris-Cohen, A. J. Think outside the (particle-in-a-)box. *J. Phys. Chem. Lett.* **2012**, *3*, 18–26.

31 Frederick, M. T.; Weiss, E. A. Relaxation of exciton confinement in CdSe quantum dots by modification with a conjugated dithiocarbamate ligand. *ACS Nano* **2010**, *4*, 3195–3200.

32 Frederick, M. T.; Cass, L. C.; Amin, V. A.; Weiss, E. A. A molecule to detect and perturb the confinement of charge carriers in quantum dots. *Nano Lett.* **2011**, *11*, 5455–5460.

33 Frederick, M. T.; Amin, V. A.; Swenson, N. K.; Ho, A.; Weiss, E. A. Control of exciton confinement in quantum dot–organic complexes through modulation of the energetic alignment of interfacial orbitals. *Nano Lett.* **2013**, *13*, 287–292.

34 Frederick, M. T.; Amin, V. A.; Weiss, E. A. The optical properties of strongly coupled quantum dot–ligand systems. *J. Phys. Chem. Lett.* **2013**, *4*, 634–640.

35 Kalyuzhny, G.; Murray, R. W. Ligand effects on optical properties of CdSe nanocrystals. *J. Phys. Chem. B* **2005**, *109*, 7012–7021.

36 Munro, A. M.; Ginger, D. S. Photoluminescence quenching of single CdSe nanocrystals by ligand adsorption. *Nano Lett.* **2008**, *8*, 2585–2590.

37 Guyot-Sionnest, P.; Shim, M.; Matranga, C.; Hines, M. Intraband relaxation in CdSe quantum dots. *Phys. Rev. B* **1999**, *60*, R2181–R2184.

38 Murphy, C. J.; Lisensky, G. C.; Leung, L. K.; Kowach, G. R.; Ellis, A. B. Photoluminescence-based correlation of semiconductor electric field thickness with adsorbate Hammett substituent constants. Adsorption of aniline derivatives onto cadmium selenide. *J. Am. Chem. Soc.* **1990**, *112*, 8344–8348.

39 Meyer, G. J.; Leung, L. K.; Yu, J. C.; Lisensky, G. C.; Ellis, A. B. Semiconductor olefin adducts. Photoluminescent properties of cadmium sulfide and cadmium selenide in the presence of butenes. *J. Am. Chem. Soc.* **1989**, *111*, 5146–5148.

40 Knowles, K. E.; Tice, D. B.; McArthur, E. A.; Solomon, G. C.; Weiss, E. A. Chemical control of the photoluminescence of CdSe quantum dot-organic complexes with a series of p-substituted aniline ligands. *J. Am. Chem. Soc.* **2010**, *132*, 1041–1050.

41 Koole, R.; Schapotschnikow, P.; de Mello Donega, C.; Vlugt, T. J. H.; Meijerink, A. Time-dependent photoluminescence spectroscopy as a tool to measure the ligand exchange kinetics on a quantum dot surface. *ACS Nano* **2008**, *2*, 1703–1714.

42 Knowles, K. E.; McArthur, E. A.; Weiss, E. A. A multi-timescale map of radiative and nonradiative decay pathways for excitons in CdSe quantum dots. *ACS Nano* **2011**, *5*, 2026–2035.

43 Bawendi, M. G.; Wilson, W. L.; Rothberg, L.; Carroll, P. J.; Jedju, T. M.; Steigerwald, M. L.; Brus, L. E. Electronic structure and photoexcited-carrier dynamics in nanometer-size CdSe clusters. *Phys. Rev. Lett.* **1990**, *65*, 1623–1626.

44 Asbury, J. B.; Hao, E.; Wang, Y.; Lian, T. Bridge length-dependent ultrafast electron transfer from re polypyridyl complexes to nanocrystalline TiO_2 thin films studied by femtosecond infrared spectroscopy. *J. Phys. Chem. B* **2000**, *104*, 11957–11964.

45 Knowles, K. E.; Malicki, M.; Parameswaran, R.; Cass, L. C.; Weiss, E. A. Spontaneous multielectron transfer from the surfaces of PbS quantum dots to tetracyanoquinodimethane. *J. Am. Chem. Soc.* **2013**, *135*, 7264–7271.

46 Malicki, M.; Knowles, K. E.; Weiss, E. A. Gating of hole transfer from photoexcited PbS quantum dots to aminoferrocene by the ligand shell of the dots. *Chem. Commun.* **2013**, *49*, 4400–4402.

47 Morris-Cohen, A. J.; Vasilenko, V.; Amin, V. A.; Reuter, M.; Weiss, E. A. A model for binding of ligands to colloidal quantum dots with concentration-dependent surface structure. *ACS Nano* **2012**, *6*, 557–565.

48 Morris-Cohen, A. J.; Frederick, M. T.; Cass, L. C.; Weiss, E. A. Simultaneous determination of the adsorption constant and the photoinduced electron transfer rate for a CdS quantum dot-viologen complex with transient absorption spectroscopy. *J. Am. Chem. Soc.* **2011**, *133*, 10146–10154.

49 Tachiya, M. Application of a generating function to reaction-kinetics in micelles - kinetics of quenching of luminescent probes in micelles. *Chem. Phys. Lett.* **1975**, *33*, 289–292.

50 Song, N.; Zhu, H.; Jin, S.; Zhan, W.; Lian, T. Q. Poisson-distributed electron-transfer dynamics from single quantum dots to C_{60} molecules. *ACS Nano* **2011**, *5*, 613–621.

51 Knowles, K. E.; Malicki, M.; Weiss, E. A. Dual-pathway photoinduced electron transfer from PbS quantum dots to a molecular acceptor. *J. Am. Chem. Soc.* **2012**, *134*, 12470–12473.

52 Knowles, K. E.; Tagliazucchi, M.; Malicki, M.; Swenson, N. K.; Weiss, E. A. Electron transfer as a probe of the permeability of organic monolayers on the surfaces of colloidal PbS quantum dots. *J. Am. Chem. Soc.* **2013**, submitted for publication.

53 Fu, X.; Pan, Y.; Wang, X.; Lombardi, J. R. Quantum confinement effects on charge-transfer between PbS quantum dots and 4-mercaptopyridine. *J. Chem. Phys.* **2011**, *134*, No. 024707.

54 Rinehart, J. D.; Weaver, A. L.; Gamelin, D. R. Redox brightening of colloidal semiconductor nanocrystals using molecular reductants. *J. Am. Chem. Soc.* **2012**, *134*, 16175–16177.

55 Tagliazucchi, M.; Tice, D. B.; Sweeney, C. M.; Morris-Cohen, A. J.; Weiss, E. A. Ligand-controlled rates of photoinduced electron transfer in hybrid CdSe nanocrystal/poly(viologen) films. *ACS Nano* **2011**, *5*, 9907–9917.

56 Hostetler, M. J.; Stokes, J. J.; Murray, R. W. Infrared spectroscopy of three-dimensional self-assembled monolayers: N-alkanethiolate monolayers on gold cluster compounds. *Langmuir* **1996**, *12*, 3604–3612.

57 Porter, M. D.; Bright, T. B.; Allara, D. L.; Chidsey, C. E. D. Spontaneously organized molecular assemblies. 4. Structural characterization of normal-alkyl thiol monolayers on gold by optical ellipsometry, infrared-spectroscopy, and electrochemistry. *J. Am. Chem. Soc.* **1987**, *109*, 3559–3568.